IOP Conf. Series: Journal of Physics: Conf. Series **851** (2017) 012029 doi:10.1088/1742-6596/851/1/012029

Quantitative image quality evaluation for kV cone-beam CT-based IGRT

S Y Lim and Hafiz M Zin

Advanced Medical and Dental Institute, Universiti Sains Malaysia, Bertam 13200 Kepala Batas, Pulau Pinang, Malaysia

E-mail: sylim617@gmail.com

Abstract. The objective of this study is to quantitatively evaluate the image quality of a kV cone-beam CT-based IGRT system (Elekta, XVI) using two commercial CT image quality phantoms, Catphan-600 and CIRS-062QA. Both phantoms consist of similar image quality test modules (uniformity, CT linearity and spatial resolution) but each phantom has different diameter and test pattern design. Each test module was imaged separately using an optimised cone-beam CT imaging parameter. The quality metrics of the reconstructed images were analysed using algorithms developed with MatLab. The image uniformity and the spatial resolution measured with Catphan were of 4% and 40% greater respectively, compared to those measured with CIRS phantom. The differences were due to the beam scattering and hardening originated from the CIRS phantom holder. The contrast-to-noise ratio (CNR) values measured with CIRS phantom were at least 2% higher than that of Catphan. The diameter of CIRS phantom is smaller and resulted in lower beam attenuation. The quantitative image quality assessment algorithms developed for both phantoms provided a phantom-specific set of reference values for a cone-beam CT imaging system as recommended by AAPM TG-142. Further investigation will be performed to resolve beam hardening issue arising from the CIRS phantom holder.

1. Introduction

Kilovoltage (kV) cone-beam computed tomography (CT) based image guided radiotherapy (IGRT) system is a useful tool for target localisation and patient setup verification during advanced radiotherapy treatment [1]. The kV cone-beam CT is able to distinguish soft tissues and provides volumetric images of the patient using low radiation doses [2–4]. The imaging system provides a tool to monitor patient positioning error and internal organ motion [2, 3] for immediate corrections of patient setup, in order to reduce the uncertainties of radiotherapy treatment. The performance of kV cone-beam CT system is dependent on the quality of the images obtained by the imaging system [5, 6]. Poor image quality, such as poor soft tissue contrast, will affect the accuracy in image registration between the CT reference image and the cone-beam CT image. This will result in patient setup error that lead to inaccurate treatment delivery.

The American Association of Physicist in Medicine (AAPM) task group (TG) 142 and 179 have recommended a set of quality assurance (QA) programmes to assure the kV cone-beam CT system has a consistent performance [7, 8]. TG-142 report provides a brief guideline of the QA programme and the frequency of performing the QA test. The details of the QA programme and the calculation of the image quality parameters were discussed in TG-179. The reports proposed that the value of each image quality parameter measured during commissioning of the system is served as the baseline value for the

periodical QA tests. Both reports did not provide any specific tolerance limits for the baseline values measured. This was due to the wide variety of commercially available kV cone-beam CT systems for IGRT. Each system is of different design and provides different imaging performance. Hence it is impossible to provide a universal quantitative tolerance limits for every image quality parameter. Besides, the quantitative metrics are also affected by the image quality phantom used to evaluate the quality metrics. To address the issues, a system-specific and phantom-specific tolerance limits are required for each IGRT system in the clinic.

In the year 2008, Bissonnette *et al.* established a set of system-specific tolerance limits for two kV cone-beam CT system according to TG-142 [3]. However, to the best of author knowledge, no research has been done in developing a phantom-specific tolerance limits for kV cone-beam CT system. To resolve the issue, this study was performed to evaluate the image quality of a kV cone-beam CT-based IGRT system quantitatively using two commercial CT image quality phantoms. The phantoms were scanned with an optimised cone-beam CT imaging parameters. A set of algorithms was developed to analyse the image quality metrics of the reconstructed images.

2. Materials and Methods

2.1. kV cone-beam CT system

The study was performed on an on-board kV cone-beam CT system, X-ray volumetric imaging (XVI) system (Elekta Oncology System, Crawley, UK), mounted on an Elekta Synergy linear accelerator platform. The XVI system consists of a kV x-ray tube and an amorphous silicon flat-panel imager that are attached on a retractable arm perpendicular to the megavoltage beam treatment head. The flat-panel imager has an active area of 41 x 41 cm^2. It comprises of 1024 x 1024 detector elements of 16-bit pixel depth and a primary filtration of 6.8 mm Al equivalence. In this study, the phantoms were scanned with an optimised imaging protocol, which captured 660 projection images in a single rotation at a frame rate of 5.5 frames per second. The field-of-view (FOV) collimator selected was S10 (27.68 cm x 13.53 cm) and the beam energy was set at 120 kVp and 0.4 mAs per projection. The scanned images were then reconstructed using Feldkamp 3D filtered back-projection reconstruction algorithm.

2.2. Phantoms

The imaging performance of the kV cone-beam CT system was evaluated using Catphan-600 (The Phantom Laboratory, Salem, NY) and CIRS-062QA (CIRS, Norfolk, VA) image quality phantom. Catphan-600 is a cylindrical phantom with a diameter of 20.0 cm and a length of 19.5 cm (Figure 1a). It is constructed of Acrylic and consists of five test modules, including CT linearity test modules, beads geometry test module, high-contrast spatial resolution test module, low contrast spatial resolution test module and uniformity test module. Whereas, CIRS-062QA phantom is smaller than Catphan-600 with a diameter of 18.0 cm and a length of 10.0 cm (Figure 2a). It also consists of all the test modules in Catphan-600 except the beads geometry test modules. Figure 1(b-f) and 2(b-e) show the reconstructed CT slice of each test module for both phantoms. Each CT slice was used to assess a specific image quality parameter. For instances, uniformity metric was evaluated with the uniformity test module, contrast-to-noise ratio (CNR) and low contrast visibility were assessed with the CT linearity test module, and the high-contrast spatial resolution was assessed with the high-contrast spatial resolution test module.

In this study, each test module was scanned separately. The phantom was positioned on the treatment couch at the gantry end. The alignment marker of the specific test module was aligned with the room laser to position the test module at the centre of the imaging system. The scanned images were reconstructed using an optimised reconstruction algorithm and exported as DICOM files. A set of algorithms was developed using MatLab (The MathWorks, Natick, MA) to evaluate the image quality metrics of the reconstructed images.

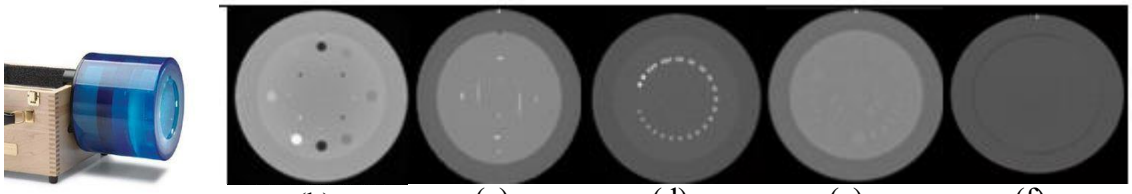

(a) (b) (c) (d) (e) (f)

Figure 1. (a) Catphan-600 phantom and the reconstructed image of each module: (b) CT number linearity test module (c) bead geometry test module, (d) high-contrast spatial resolution test module, (e) low-contrast spatial resolution test module and (f) uniformity test module.

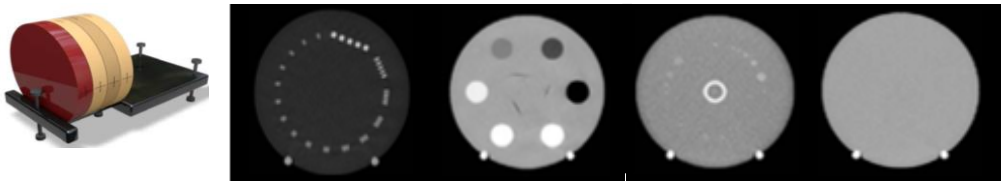

(a) (b) (c) (d) (e)

Figure 2. (a) CIRS-062QA image quality phantom and the reconstructed image of each test modules: (b) high-contrast spatial resolution test modules, (c) CT number linearity test modules, (d) low-contrast spatial resolution test modules, and (e) uniformity test modules.

2.3. Image evaluation

Image uniformity was determined based on pixel values across the centre of the uniformity CT slice in the vertical and the horizontal directions. A region of interest (ROI) of a height of 10.0 mm and a width that covered 80% of the phantom from the centre point was selected for both vertical and horizontal directions. The mean pixel values, $\bar{x}$, across the columns of the ROIs were calculated and a uniformity profile was plotted for both vertical and horizontal axes. The mean pixel values were also used to determine the integral non-uniformity values using equation (1).

$$\text{Integral non-uniformity} = \left(\frac{\max(\bar{x})-\min(\bar{x})}{\max(\bar{x})+\min(\bar{x})}\right) \quad (1)$$

The contrast-to-noise ratio (CNR) and low contrast visibility were evaluated using the CT number linearity module. In Catphan-600, the CT linearity test module consists of several cylindrical inserts made of different materials, such as Polystyrene, low-density polyethylene (LDPE), Acrylic, Delrin, Teflon, air and polymethylpentene (PMP), of known electron densities and CT numbers. Whereas, for CIR-062QA phantom, the test module contains all the inserts in Catphan-600, except PMP, in a greater diameter of 25.4 mm (Figure 2c). A ROI of 3.5 x 3.5 mm^2 was selected within each insert. The mean pixel values, $\overline{x}_i$, and the standard deviation, $\overline{\sigma}_i$, of each ROIs was calculated. Another ROI of the same size as the insert ROI was selected for each insert to calculate the mean pixel value of background, $\overline{x}_{bg}$, and the corresponding standard deviation, $\overline{\sigma}_{bg}$. The CNR value was calculated using equation (2). The CNR is defined as the difference of mean pixel values between the insert and the corresponding background over the averaged noise [11].

$$\text{CNR} = 2 \times \left[\frac{|\overline{x}_i-\overline{x}_{bg}|}{\overline{\sigma}_i+\overline{\sigma}_{bg}}\right] \quad (2)$$

Low contrast visibility was determined using the Polystyrene insert and the LDPE insert. The low contrast visibility value was computed based on the corresponding mean and pixel value of the inserts using equation (3) [5, 6],

$$\text{Low contrast visibility} = \frac{(CT_{poly}-CT_{LDPE})/10}{(\overline{x}_{poly}-\overline{x}_{LDPE})/(\frac{1}{2})(\sigma_{poly}-\sigma_{LDPE})} = \frac{2.75(\sigma_{poly}-\sigma_{LDPE})}{\overline{x}_{poly}-\overline{x}_{LDPE}} \quad (3)$$

where CT_{poly} and CT_{LDPE} represents the CT number of Polystyrene and LDPE inserts, $\overline{x}_{poly}$ and $\overline{x}_{LDPE}$ represent the corresponding mean pixel values, while σ_{poly} and σ_{LDPE} represent the corresponding standard deviation values of each insert. The factor of 2.75 is the calculated difference between Polystyrene and LDPE in CT numbers.

The spatial resolution of the kV cone-beam CT system was determined using the high-contrast spatial resolution test module. In Catphan-600, the spatial resolution test module consists of aluminium bar patterns of spatial frequencies ranging from 1-21 lp/cm, whereas, in CIRS-062 QA phantom, the range of spatial frequencies are from 1-16 lp/cm. Besides, the thickness of the aluminium bar in CIRS-062QA phantom is 10.0 mm greater than that in Catphan-600 of only 2 mm. The spatial resolution was evaluated in terms of modulation transfer function (MTF) values. The MTF value of each bar pattern was calculated by using the Droege and Morin method [10]. With the obtained results, an MTF curve was plotted. Among the MTF values, *f*50 and *f*10 are the important values because *f*50 indicates the point where human perceive an image to be sharp; while *f*10 is the highest resolution limit which the human eye can possibly differentiate the bar patterns. The spatial frequencies corresponding to *f*50 and *f*10 were determined from the MTF curve.

3. Results and discussion

Figure 3 shows the uniformity profiles in both horizontal and vertical directions for Catphan-600 and CIRS-062QA phantom. The results obtained with Catphans-600 show a greater image uniformity compared to CIRS-062QA. This is reflected in the integral non-uniformity obtained, where the integral non-uniformity of Catphan-600 was 0.0163 and the corresponding results for CIRS-062QA was 0.0504. The lower the integral non-uniformity values, the better the image uniformity. Besides, there is a presence of cupping artefact in the image acquired with CIRS-062QA phantom, where the mean pixel value is the lowest in the central region of the phantom (Figure 3).

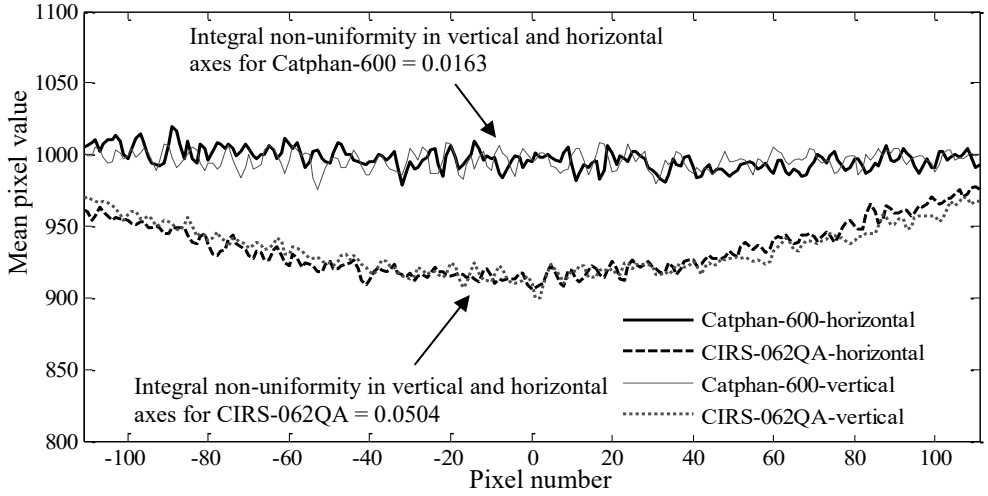

Figure 3. The uniformity profiles across the images in the horizontal and the vertical axis for both phantoms.

The cupping artefact is due to the beam scattering and hardening yielded from the phantom holder. According to the manufacturer, the phantom holder is made of a non-water equivalent material, which has a CT number higher than water. Moreover, due to the limitation of the collimator setting and the extension of the phantom holder, the captured projection images of the uniformity test module had included some parts of the phantom holder, such as the screw (Figure 4a), and hence resulted in greater scattering and beam hardening that in turn caused the presence of the cupping artefact, as shown in figure 4b.

In the evaluation of the contrast metrics, CNR values of each insert in CIRS-062QA are of 2% - 184% higher compared to those of Catphan-600 (Figure 4a). The mean pixel values obtained within each insert in CIRS-062QA phantom are of 8% - 59% greater than those that measured with Catphan-

600. While, the standard deviation values from CIRS-062QA phantom are 1%-40% lower than Catphan-600. These have resulted in lower CNR values in CIRS that contributed from the size of CIRS-062QA phantom that is 1.4 time smaller than Catphan-600. The smaller the phantom size, the lower the beam attenuation and the image noise and in turn increased the CNR value.

CIRS-062QA phantom yielded a lower low contrast visibility value of 1.83 compared to that of Catphan-600 of 2.42. CIRS-062QA phantom is smaller than Catphan-600, and resulted less attenuation of beam and reduction of image noise. Low contrast visibility is directly proportional to the image noise. The lower value indicates the lesser presence of the image noise and better visualisation of soft tissue for CIRS-062QA phantom compared to Catphan-600.

The MTF results obtained with both phantoms are plotted in Figure 5b. The spatial frequencies obtained with Catphan-600 at *f*50 and *f*10 were 5.26 lp/cm and 9.24 lp/cm, respectively. The corresponding results for CIRS-062QA phantom were 4.08 lp/cm for *f*50 and 6.63 lp/cm for *f*10. The spatial resolution of a CT imaging system is dependent on the focal spot size, the voxel size, the type of x-ray scintillator and the number of the projection images [11]. In this work, both phantoms were scanned using the same imaging parameters to eliminate the dependency to the aforementioned factors. The discrepancy in spatial resolution might be because of the spatial resolution test module design and the material used in constructing the test module. The difference in aluminium bar thickness and background material formulation used for both Catphan-600 and CIRS-062QA phantom generate different level of beam attenuation and image visibility and hence affect the spatial resolution of the reconstructed CT image.

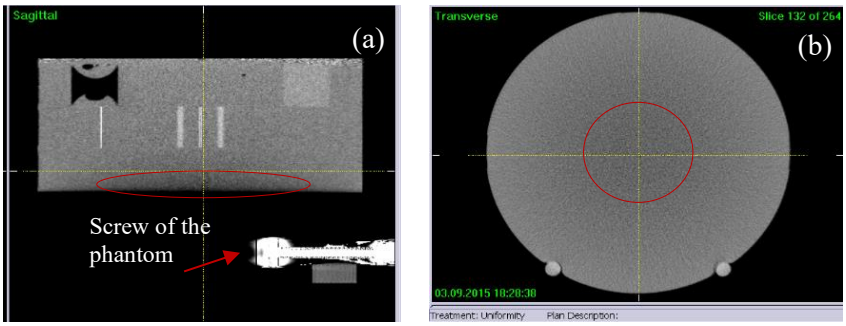

Figure 4. Photo of the reconstructed image (a) in the sagittal view and (b) in the transverse view. The circled regions show a higher grayscale value due to the beam hardening originated from the screw and the phantom holder.

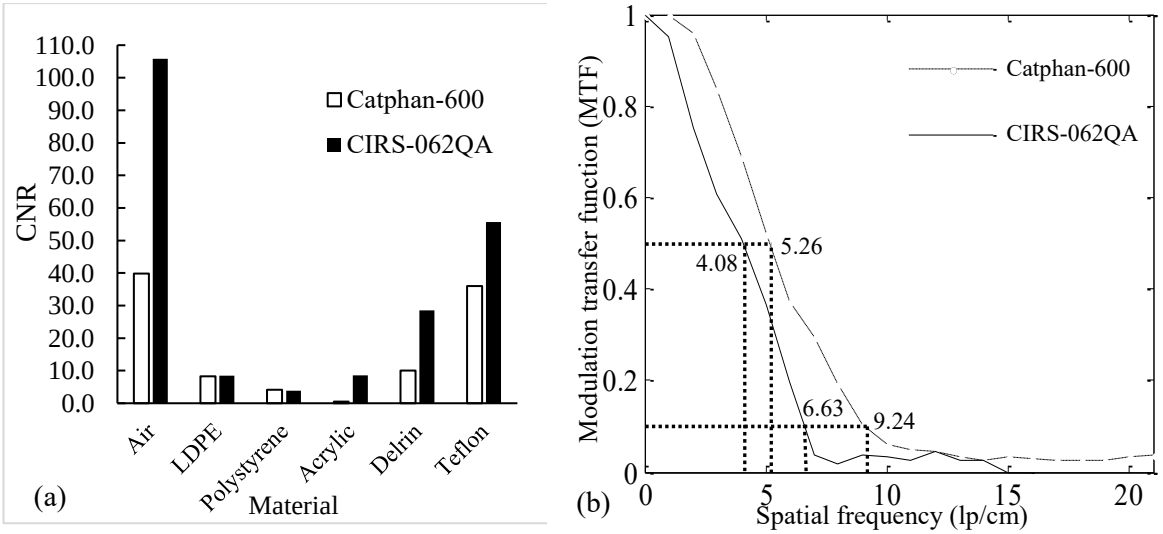

Figure 5. a) The CNR values for different materials determined by using Catphan-600 and CIRS-062QA phantom. (b)The modulation transfer function (MTF) obtained with both Catphan-600 and CIRS-062QA phantom.

Overall, the image quality results obtained with Catphan-600 are within the tolerance of the imaging system specification and consistent with that from Bissonnette *et al*. (2008) [3]. According to Bissonette et al. (2008) study, the reported integral non-uniformity value for Catphan-600 is ranging from 0.009-0.039; while the tolerance limit of spatial frequency at *f*10 is between 4.6 lp/cm and 9.9 lp/cm.

In summary, this research work has provided a phantom-specific baseline values for each image quality metric of the kV cone-beam CT system. Apart from image uniformity, the difference of other image quality parameters between both phantoms are due to the size and the design of the phantoms. The image uniformity measured with the CIRS-062QA phantom can be improve by eliminating the beam scattering and hardening originated from the screws and the phantom holders. Further investigation on resolving this issue will be performed.

4. Conclusion

Image quality metrics of a kV cone-beam CT system were assessed using two commercial phantoms. The algorithms developed for the quantitative image quality evaluation provides a phantom-specific set of reference value for a kV cone-beam CT system. The variations of image quality metrics between the phantoms were due to the difference in the size and the geometric design of the phantoms. Future work will focus on improving the setup of the CIRS-062QA phantom, in order to exclude the screws and the phantom holder from the field-of-view of the collimator during scanning.

5. References

[1] Stützel J, Oelfke U and Nill S 2008 A quantitative image quality comparison of four different image guided radiotherapy devices *Radiother. Oncol.* **86** 20–4.
[2] Bissonnette J, Moseley DJ, Jaffray D A 2008 A quality assurance program for image quality of cone-beam CT guidance in radiation therapy *Med. Phys.* **35** 1807–15.
[3] Garayoa J, Castro P 2013 A study on image quality provided by a kilovoltage cone-beam Computed tomography *J. Appl. Clin. Med. Phys.* **14** 239–57.
[4] Alaei P, Spezi E 2015 Imaging dose from cone beam computed tomography in radiation therapy *Phys. Med*. **31** 647-58
[5] Nakahara S, Tachibana M, Watanabe Y 2016 One-year analysis of Elekta CBCT image quality using NPS and MTF *J. Appl. Clin. Med. Phys.* **17** 6047.
[6] Stock M, Pasler M, Birkfellner W, Homolka P, Poetter R and Georg D 2009 Image quality and stability of image-guided radiotherapy (IGRT) devices: A comparative study *Radiother. Oncol.* 2009 **93** 1–7.
[7] Klein E, Hanley J, Bayouth J, Yin F, Simon W, Dresser S, Serago C, Aguirre F, Ma L, Arjomandy B, Liu C, Sandin C and Holmes T 2009 Task Group 142 report: quality assurance of medical accelerators *Med. Phys*. **36** 4197–4212.
[8] Bissonnette J, Balter P, Dong L, Langen K, Lovelock D, Miften M, Moseley D, Pouliot J, Sonke J and Yoo S 2012 Quality assurance for image-guided radiation therapy utilizing CT-based technologies: A report of the AAPM TG-179 *Med. Phys.* **39** 1946-63.
[9] Droege RT and Morin RL 1982 A practical method to measure the MTF of CT scanners *Med. Phys.* **9** 758–760.
[10] Shaw CC 2014. *Cone Beam Computed Tomography* (New York: CRC Press)
[11] U. Elstrøm, L. Muren, J. Petersen and C. Grau 2011 "Evaluation of image quality for different kV cone-beam CT acquisition and reconstruction methods in the head and neck region", *Acta Oncologica* **50** 908-917.

Acknowledgments

Lim Siew Yong studentship is funded by MyBrain15scholarship. This research is funded by Fundamental Research Grant Scheme, Ministry of Education Malaysia, 203/CIPPT/6771383. The authors would like to thank the radiotherapists in the Radiotherapy & Oncology Unit, AMDI, USM for the help given in this research.